11th International Conference on Fracture Mechanics of Concrete and Concrete Structures
FraMCoS-11
J. M. Chandra Kishen, A. Ramaswamy, S. Ray and R. Vidyasagar (Eds)
https://doi.org/10.21012/FC11.092370

PREDICTIVE POWER OF CRACK OPENING RATE FOR FLEXURAL FATIGUE LIFE OF STEEL FIBRE-REINFORCED HIGH AND ULTRA-HIGH PERFORMANCE CONCRETE

G. GEBUHR[*], Á. MENA-ALONSO[†], M. PISE[‡], S. ANDERS[*], M.A. VICENTE[†], D. BRANDS[‡] AND J. SCHRÖDER[‡]

[*] Institute of Structural Engineering, Faculty of Architecture and Civil Engineering,
Bergische Universität Wuppertal, Wuppertal, Germany
Corresponding Author Email: gebuhr@uni-wuppertal.de

† Department of Civil Engineering, University of Burgos, Burgos, Spain
C. Villadiego s/n, 09001 Burgos, Spain

‡ Institute of Mechanics, Faculty of Engineering, Universität Duisburg-Essen, Essen, Germany
Universitätsstraße 15, 45141 Essen, Germany

Key words: (Ultra-)High Performance Concrete, Steel fibres, Deterioration, Fatigue, Multi-level Loading, Cycle Jump Technique

Abstract: Numerical modelling of deterioration in high-cycle fatigue is limited primarily by the computational time required to explicitly calculate large numbers of load cycles on a specific system. Therefore, the aim of this work is to develop an experimentally driven approach to predict the damage evolution of notched 3-point bending beams specimens made of fibre-reinforced high- and ultra-high-performance concrete (HPC/UHPC), which can be used to limit the necessity of extensive numerical calculations of such tests. One possible application is cycle-jump approaches, which aim to avoid the explicit calculation of a large part of the load cycles up to the fatigue failure of the system in the numerical calculations – without having to accept significant losses in the predictive capability of the model. In this contribution, the predictive capability of the crack mouth opening displacement rate ΔCMOD per load-cycle in the second phase of fatigue onto the overall fatigue damage progression is characterised for flexural beams. In this case, this is not explicitly linked only to final failure of the structure. The outlined approach can also be used to estimate the number of cycles until a specifically defined CMOD is reached. This can be important, for example, if crack widths may not be exceeded in cyclically loaded structures. In addition to reference specimens of extremely brittle UHPC and HPC without fibres, the test program consists of specimens with fibre contents of 0.75 % and 1.5 % by volume, which show strain-hardening behaviour. I.e., in preliminary tests, the bending tensile strength was only reached after the proportional limit was reached. The experimental programme includes numerous fatigue tests with constant lower and upper load levels as well as multi-level tests in which one or both load levels were gradually shifted in a block-wise manner. For each block, the cyclic loading was applied long enough to reach the second, linear phase of fatigue deterioration. Overall, it is shown that the secondary creep rate in terms of crack mouth opening provides a valid basis for predicting the failure time (or reaching a given CMOD), despite the well-known scatter of fatigue test series. In a brief outlook, the applicability of a similar use of the stiffness development of the test specimens as a means of prognosis is additionally discussed.

1 INTRODUCTION AND STATE OF THE ART

A key trend in modern construction industry is the ongoing increase in demands on cementitious building materials. However, the development of high-strength and ultra-high-strength concretes (HPC and UHPC) also leads to new challenges, particularly with regard to ductility, fatigue behaviour and brittleness, see e.g. [1–5]. A central approach to counteracting these problems is the addition of steel fibres to the concrete mix. Although conventional normal-strength concrete already is a highly heterogeneous composite material, its complexity is further increased when adding fibres. This directly complicates e.g. computer-aided description of the structural behaviour of such materials through numerical modelling. However, it is possible to model this material, as shown in [6,7], for a limited number of cycles, the limiting factor for simulation of high-cycle fatigue is computational power. The focus of previous work was therefore on the transferability of the material behaviour of (ultra-)high performance concrete in quasi-static loading to fatigue loading. For this purpose, different damage indicators such as the development of the crack opening displacement (CMOD) or the residual stiffness (s) were analysed, see e.g. [8] and [9].

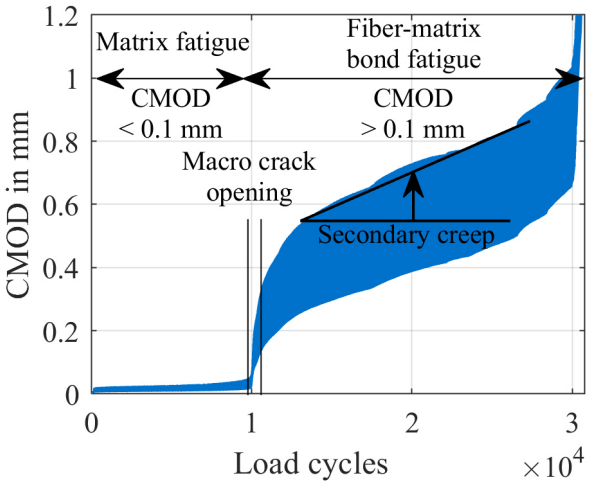

Figure 1: Flexural fatigue of steel fibre reinforced HPC with distinct matrix fatigue (CMOD < 0.1mm) and fibre-matrix bond fatigue (CMOD > 0.1mm).

Another important step in the numerical description of degradation is the way damage accumulates throughout fatigue loading. For consideration of several successive load blocks in terms of damage accumulation hypothesis, e.g. the Palmgren-Miner hypothesis, see [10], and in extension Paris' law, see [11], offer basic approaches to the description of damage growth. Here, the focus is on the development of damage in the so-called secondary creep phase. Figure 1 illustrates these ideas using the example of fatigue of a steel fibre reinforced beam in flexure also relating it to the underlying research presented in this paper.

Fatigue is classically divided into a three-phase process. The second phase, indicated by roughly linear damage accumulation, is commonly referred to as secondary creep phase. In the present case, the inserted fibres can develop a large part of their load-bearing effect after the surrounding matrix has failed due to large deformations, such as the occurrence of matrix cracks. This effectively results in two consecutive fatigue processes. First, the concrete matrix fatigues at small deformations, then cyclic loading of the fibre-matrix bond following the macro-crack opening. Both fatigue processes have their own secondary creep phase, with significantly different gradients of degradation.

In literature, steel fibre reinforced concrete is usually investigated in uniaxial compression and tensile tests, e.g. [12,13], as well as in flexural tests, e.g. [9,14], with regard to the secondary creep rate.

The aim of the present research work is to provide an examination of the degradation process as a function of different loading scenarios and histories in fatigue for HPC and UHPC with different steel fibre contents. For this purpose, primarily the secondary creep rate ΔCMOD is considered. These results are aimed to be aid in cycle-jump approaches as a means to accelerate the calculation process by selectively eliminating certain cycles by “cycle jumping” from explicit calculations while still providing reasonably accurate results.

2 MATERIALS

The experiments were conducted on one high strength (HPC) and one ultra-high strength (UHPC) concrete mix. Both recipes as shown in Table 1 were designed to be used as reference mixtures within the German DFG Priority Programme SPP 2020. They are therefore being investigated in various research projects with regard to different material properties with a main focus on fatigue behaviour, e.g. in [15,16].

Table 1: Mixtures of the investigated concretes.

Ingredient	HPC kg/m³	UHPC kg/m³
CEM I 52.5R	500	795
Quartz powder	-	198
Fine sand	75	971
Sand 0/2	850	-
Basalt 2/5	350	-
Basalt 5/8	570	-
Silica fume	-	169
Superplasticizer	5	24
Stabilizer	3	-
Water	176	188
Steel fibres	0 / 57 / 115	0 / 57 / 115

Both concretes were tested as plain concrete as well as containing two different fibre contents. The size of the fibres was chosen based on the aggregate grain size of each mixture. Consequently, for the HPC with a maximum grain size of 8 mm, hooked-end macro-fibres with a diameter of 0.92 mm, a total length of 60 mm and a tensile strength of 1160 N/mm² were chosen. In case of the UHPC, which has a significantly smaller maximum grain size of 0.5 mm, smooth micro-fibres with a diameter of 0.19 mm, a length of 13 mm, and a tensile strength of about 2000 N/mm² were used.

The HPC mixture has a 28-day compressive strength of 102 N/mm², the UHPC reaches a compressive strength of about 160 N/mm², see [17] and [9], respectively.

3 EXPERIMENTAL PROGRAMME

All tests were carried out on notched beams in flexure with dimensions of 150 x 150 x 700 mm³.

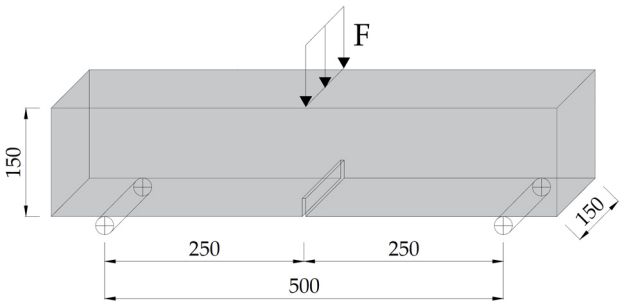

Figure 2: Schematic test setup.

The test setup, depicted in Figure 2, follows DIN EN 14651 for the determination of fibre performance in static flexural tests.

As mentioned, a sequence of fatigue loads varied in blocks in upper and lower load levels was applied to each test specimen. Each combination of load levels was applied for a minimum of 10^5 loading cycles or until the specimen experienced structural failure.

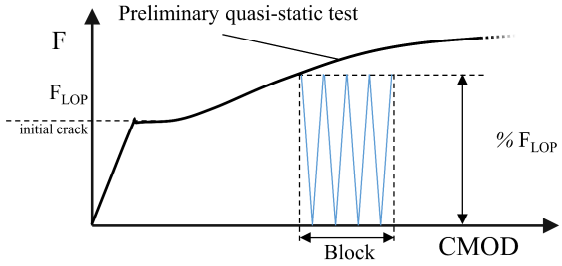

Figure 3: exemplary part of an envelope of a preliminary quasi-static test, see [6], definition of F_{LOP} and loading block.

The load levels were determined as fractions of the level of proportionality F_{LOP} as depicted in Figure 3. This reference load was derived in preliminary quasi-static tests. For HPC, these tests are comprehensively discussed in previous work, see [6].

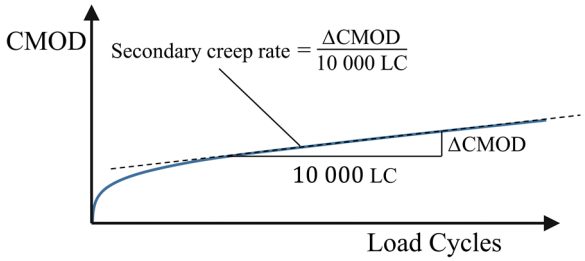

Figure 4: Definition secondary creep rate in a single block.

The focus of the investigations presented here is on the consideration of the secondary creep rate at certain fatigue loads or the gradient of the crack opening. The definition is sketched in Figure 4.

The testing program included separate tests for the combined examination of matrix and fibre-matrix bond fatigue as well as pre-cracked-tests in which only the latter was examined. To omit time-consuming matrix fatigue, specimens were statically pre-cracked to a crack mouth opening of about 0.1 mm.

For an overview of the applied load levels, refer to Table 2 and the accompanying Figure 5.

Table 2: Investigated loading schemes.

	Load schemes
Tests including matrix fatigue	a (including single Block tests with constant F_{upper})
Tests skipping matrix fatigue (static loading to 0.1 mm CMOD)	a, b, c, d

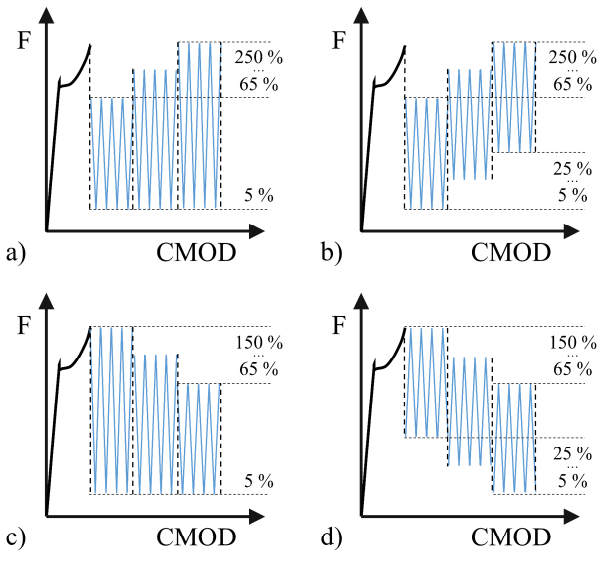

Figure 5: Investigated loading schemes, accompanying overview for Table 1. Percentages given are in % of F_{LOP}

It should be noted that due to the rather high fibre contents considered, there is a highly smooth transition from matrix fatigue to fibre-matrix bond fatigue. Therefore, in case of these supercritical fibre contents showing strain-hardening behaviour, the required upper load levels F_{upper} to achieve a crack opening of 0.1 mm can be higher than 100 % of F_{LOP}.

4 RESULTS AND DISCUSSION

4.1 Presentation methodology

In the following, the correlation between the load levels applied during fatigue tests and the corresponding development in crack opening ΔCMOD per 10 000 load cycles is analyzed. As mentioned, load levels are given as a percentages of the force F_{LOP} determined as limit of proportionality in quasi-static preliminary tests on beams made of the same concrete and with the same fibre content. An overview of the reference loads applied for F_{LOP} can be found in Table 3.

Table 3: Reference load levels for F_{LOP}.

Concrete	Fibre Content kg/m³	F_{LOP} kN
HPC	0	14.6
	57	20.1
	115	21.1
UHPC	0	19.1
	57	23.1
	115	24.0

Generally, a logarithmic relationship between the applied load level and degradation rate is expected and indicated accordingly.

Despite the unavoidable scatter commonly observed in fatigue testing, the results cluster depending on the fibre quantities with regard to the rate of degradation. Rather than the more usual indication of a linear regression of the results, a visualization grouping the results as clusters utilizing confidence ellipses as described in [18] came into application. This way, the differentiation of the resulting areas of experiments of different types becomes better distinguishable. The confidence ellipses are characterized by their semi-axes, which represent the standard deviation of the largest and smallest scatter direction. The longer semi-axis is equal to the linear logarithmic regression. Thus, it provides a main indicator

for the approximation of the degradation for cycle-jump approaches. It should further be noted that the semi-axes of the confidence ellipses cannot be read directly from the graphs due to distortion of the representtation caused by the different scaling of the x- and y-axes. Therefore, the increase of the longer semi-axis is additionally given in accompanying tables.

4.2 Damage development during matrix fatigue (CMOD < 0.1 mm)

Figure 6 shows the fatigue behaviour of both concrete types up to a CMOD of 0.1 mm. As shown in Figure 1, this value coincides with fatigue failure of the concrete matrix.

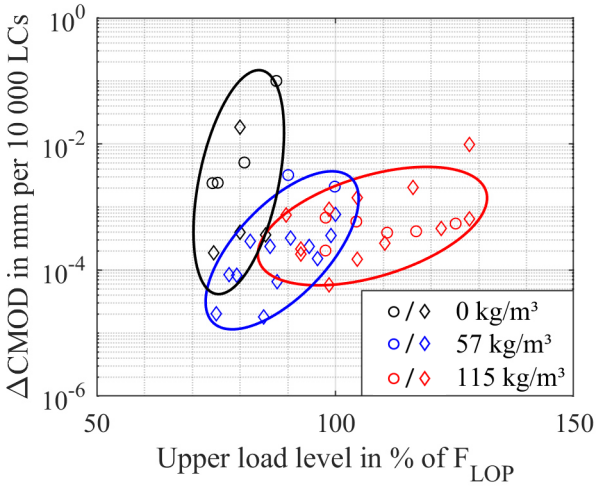

Figure 6: Overview of ΔCMOD per 10 000 load cycles during matrix fatigue (CMOD < 0.1 mm), including HPC (○) and UHPC (◊).

Table 4 displays the relative load increase, which is required to tenfold the degradation rate. It thus gives a comparative idea of the fatigue strengths regarding the fibre content.

Table 4: % of F_{LOP} necessary to increase ΔCMOD per 10 000 LCs by a factor of ten, overview for matrix fatigue with CMOD < 0.1 mm

Concrete	Fibre Content in kg/m³	F_{upper} increase to tenfold ΔCMOD in % of F_{LOP}
HPC & UHPC	0	4.5
	57	8.4
	115	23.2

It is noticeable that the results can be clustered in each case according to the amount of fibres contained, irrespective of the compressive strength of the concrete. The degradation rate given in terms of crack opening rate ΔCMOD is highest for fibre-free beams and decreases depending with an increasing amount of fibres.

Overall, it can be stated for matrix failure respectively the crack-initiation phase that the effect of fibres is clearly visible. For example, a specimen with a fibre content of 115 kg/m³ requires more than a fivefold increase in the relative upper load-level to achieve a comparable change in the damage gradient referred to concrete without fibres. It should also be noted that the clusters partially overlap. This overlapping of clusters could be partly attributed to the reference loads used in the tests, as presented in Table 4. These reference loads have the tendency to inflate values obtained for lower fibre contents, as they use lower reference loads as a basis for the percentage reference for F_{LOP}. Further research is also needed to evaluate other factors. For example, higher fibre amounts do not always guarantee larger amounts of fibres in the crack area, which in some cases could lead to comparable behaviour between samples with e.g. 57 and 115 kg/m³ fibres.

For all test specimen discussed in this section, the first block was applied for approximately 500 000 load cycles. If the sample had not formed a crack and accordingly had not yet entered fatigue of the fibre-matrix bond, the load was increased. This mainly affected beams with 115 kg/m³ fibres. Here, load levels of up to 130 % of the reference load F_{LOP} from the quasi-static tests were needed to initiate a macro-crack. This is due to the particularly smooth transition into the opening of clearly identifiable macro cracks for specimens.

4.3 Damage development during fibre-matrix bond fatigue (CMOD > 0.1 mm)

Figure 7 a) exemplarily shows the behaviour of UHPC when exceeding a crack opening of 0.1 mm. Here, only experiments conducted

with increasing upper and constant lower load levels are depicted. In Figure 7 b, this depiction is extended to all further loading schemes listed in Table 2.

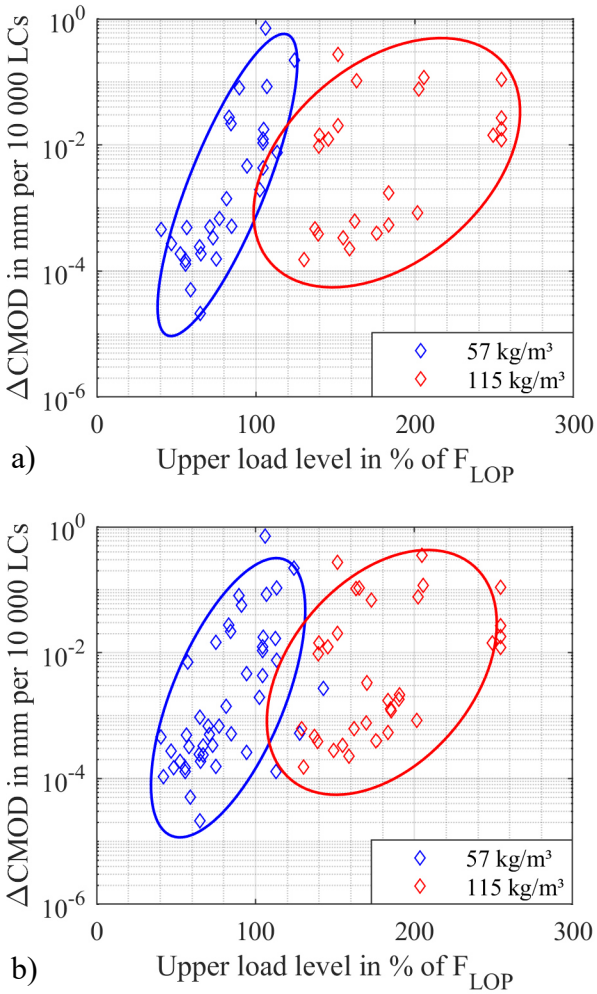

Figure 7: Overview of ΔCMOD per 10 000 LC (CMOD > 0.1 mm) during fibre-matrix bond fatigue, crack mouth opening rate ΔCMOD, UHPC, a) only static F_{lower} and increasing F_{upper}, and b) all tests.

Noticeably, the influence of fibre content is significantly higher than that of loading history. As this applies to all combinations tested. A possible influence of the load history is not explicitly considered in the following.

In addition to the tests in which the failure of was caused by fatigue loading, i.e. the direct continuation of the tests depicted in Figure 3, specimens are included which were pre-cracked statically to a crack opening of 0.1 mm before starting fatigue loading.

Again, the results are clustered according to fibre content, with specimens with higher fibre content reacting less sensitive to changes in the upper load level, but showing higher scatter.

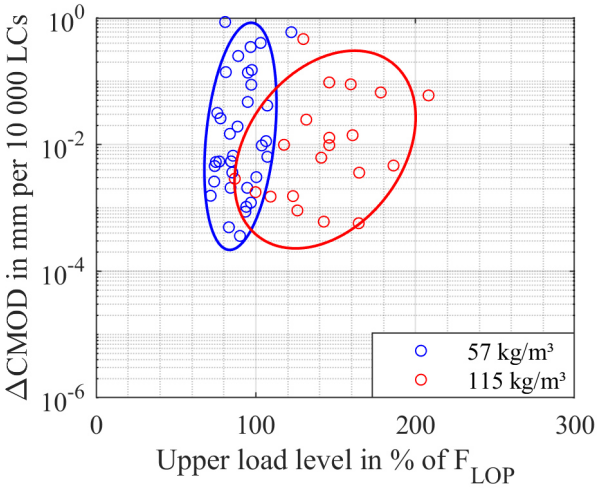

Figure 8: Overview of ΔCMOD per 10 000 load-cycles (CMOD > 0.1 mm) during fibre-matrix bond fatigue, crack mouth opening rate ΔCMOD, HPC, all tests.

As shown in Figure 8, the statements given for UHPC with micro-fibres also apply to specimens made of HPC with hooked-end macro-fibres.

Overall, in comparison to the matrix fatigue, the susceptibility of the measured growth rates of CMOD to increasing load levels decreases for both fibre contents. With a fibre content of 57 kg/m³, it should also be noted that a jump in the measured damage gradients was notable between matrix- and fibre-matrix bond fatigue at directly comparable upper load levels. Thus, at an F_{upper} of 100 % of F_{LOP}, the damage rate for HPC is on average approximately 0.5 mm per 10 000 load cycles and 0.1 mm for UHPC during fibre-matrix bond fatigue. During matrix fatigue, on average 0.01 mm per 10 000 load cycles was measured for both concrete types.

Table 5: % of F_{LOP} necessary to increase ΔCMOD per 10 000 LCs by a factor of ten, overview fibre-matrix bond fatigue.

Concrete	Fibre Content kg/m³	F_{upper} increase to tenfold ΔCMOD % of F_{LOP}
HPC	57	17.8
	115	48.2
UHPC	57	21.4
	115	73.4

Up to now, only few results are available for 115 kg/m³ fibres in the range up to 100 % of F_{LOP}, direct comparability cannot be assured here.

Overall, the test results show a soft transition between the two fatigue phases. This is most probably due to the high number of single fibres in UHPC.

Looking at the correlation between change in applied F_{upper} and corresponding change in crack opening gradient shown in Table 5, there are clear differences between the types of concrete during fibre-matrix bond fatigue. In direct comparison between the two fatigue phases, both HPC and UHPC behave less sensitive with regard to changes in the upper load level. Interestingly, the ratio of gradients between fibre contents is similar for HPC. Here, between 57 kg/m³ fibres and 115 kg/m³ fibre with 8.2 % to 23.4 % and 17.8 % to 48.2 % of F_{LOP}, respectively, to produce a tenfold increase in the rate of damage. For UHPC with micro-fibres, doubling the fibre quantity has an even stronger effect with an increase from 21.4 % to 73.4 %.

These values represent a framework in which the damage rate in the linear creep phase can be assessed and thus extrapolated and used for the calibration and evaluation of cycle-jump approaches.

5 SUMMARY AND OUTLOOK

5.1 Summary

In this paper, the influence of different amounts of steel fibres on the damage development in flexural fatigue of high and ultra-high performance concrete was examined. For this purpose, 3-point flexural bending tests with fatigue loading were carried out and the gradient of the crack opening rate ΔCMOD was examined. The range of loading schemes included blocks with different upper and lower load levels, which were applied until secondary creep was reached. In order to investigate effects of the loading history, different combinations of blocks with increasing and decreasing upper and lower load levels were considered. In addition, a distinction was made between fatigue of the matrix and fatigue of the fibre-matrix bond.

In order to focus on the clustering of results found in the experiments, confidence ellipses were given in addition to the specified logarithmic linear regression. Anhand dieser Using this data, the damage evolution of the specimens during fatigue can be estimated to predict the number of load cycles necessary to achieve specific crack openings.

Both types of concrete show a behaviour that is primarily defined by the amount of added fibres, both during matrix and in fibre-matrix fatigue. Furthermore, the steel fibres introduced significantly enhance the resistance to the increase in applied fatigue loads in all loading schemes tested.

During the fatigue loading of the matrix at CMOD's below 0.1 mm, only small but noticeable differences were observed between the fibre quantities. It can therefore be assumed that even during the second phase of fatigue, when the fatigue-typical cracking starts to appear, forces are already being transferred to the bonded fibres. After the failure of the matrix and the activation of the full fibre load-bearing effect during the fibre-matrix bond fatigue, there are correspondingly significantly greater differences in opening rate. Here, especially with higher fibre contents, significantly more pronounced scatter in the degradation of fibre-matrix bond was found. This can be attributed to e.g. casting process-related fluctuations in the fibre quantity in the critical crack area, but needs to be further investigated.

Overall, the crack opening rate ΔCMOD seems to be a suitable and sufficiently stable indicator for the evaluation and prediction of specific damage states necessary to approach cycle jumps in numerical simulation.

5.2 Outlook

In previous studies, see e.g. [6,8,9], other damage indicators were considered in addition to the assessment of the damage state in the form of the crack opening CMOD. These investigations initially focused on deformation-controlled flexural tests with a limited number of unloading and reloading cycles, see [8], each

carried out after CMOD-controlled initiation of different crack openings. The aim was to investigate the damage of these specimens using different indicators for crack-opening respectively deterioration. In a second step, force-controlled fatigue tests were carried out with the same fibre contents. It was shown that especially the consideration of the stiffness, i.e. the gradient of the force-crack opening relation of individual unloading and subsequent reloading cycles as depicted in Figure 9 a), is adequate in establishing a dependency between quasi-static and fatigue tests. As such, the residual stiffness was significantly more dependent on the respective fibre content and crack width than on the upper and lower load levels. Furthermore, it was shown in [9] that this can also be transferred to specimens with different loading histories of blocks of different load levels.

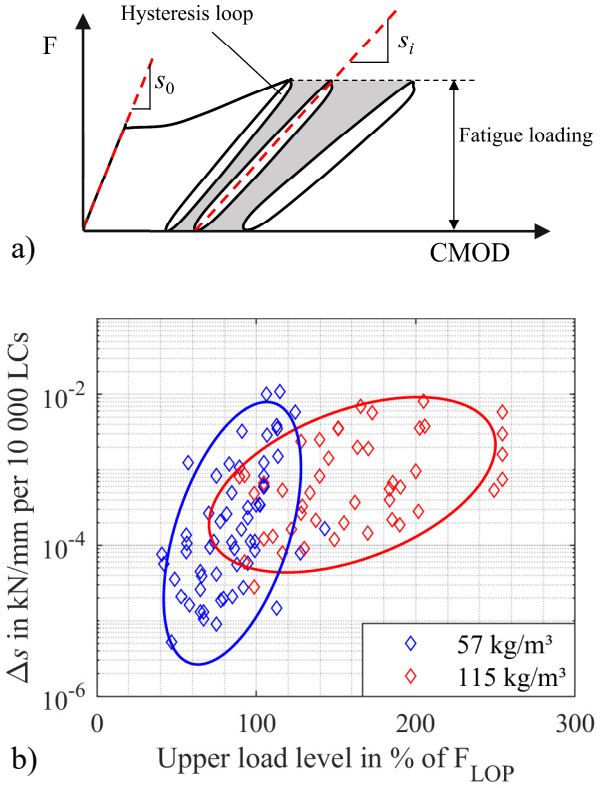

Figure 9: Stiffness deterioration rate Δs per 10 000 load-cycles, a) definition of the stiffness and b) test results of UHPC.

Figure 9 b) shows the gradient of the change in stiffness Δs of all tests presented in this contribution on UHPC previously shown with regard to ΔCMOD. Here, no differentiation is made between fatigue of the matrix and fatigue of the fibre-matrix bond. Similar to the consideration of the crack opening rate ΔCMOD, the presented tests can be clearly selected on the basis of the respective fibre content. Furthermore, the representation gives a more homogeneous picture regarding the scatter of the tests than the previously shown ΔCMOD's, especially for amounts of 115 kg/m³ fibres.

With regard to the representation of the change of CMOD at top load, as it is primarily considered by [10,11], for example, the inclusion of further indicators for the damage in view of a realistic modelling of the degradation gives correspondingly further possibilities and should also be investigated. In a next step, it is necessary to investigate additional boundary criteria that provide a framework in which the results presented here are applicable.

7 ACKNOWLEDGEMENTS

This research has been funded by the Deutsche Forschungsgemeinschaft (DFG, German Research Foundation), project number 353513049 (AN1113/2-2, BR5278/2-2, SCHR570/32-2) within the DFG Priority Programme 2020 "Cyclic deterioration of high performance concrete in an experimental-virtual lab". Furthermore, the provision of steel fibres by Bekaert and Stratec is kindly acknowledged.

8 REFERENCES

[1] Fitik B., 2012. Ermüdungsverhalten von ultrahochfestem Beton (UHPC) bei zyklischen Beanspruchungen im Druck-Zug-Wechselbereich [Ph.D Thesis]. München: Technischen Universität München.

[2] Hulett T., Clarke J., 2016. Technical report 34 (third edition) - Concrete industrial ground floors: A guide to design and construction. Surrey, UK.

[3] Benjamin A Graybeal, 2014. Design and Construction of Field-Cast UHPC Connections. Federal Highway Administration.

[4] Naaman A (ed.), 2011. HALF A CENTURY OF PROGRESS LEADING TO ULTRA-HIGH PERFORMANCE FIBER REINFORCED CONCRETE PART 1-OVERALL REVIEW. RILEM Publications SARL.

[5] Naaman A (ed.), 2011. HALF A CENTURY OF PROGRESS LEADING TO ULTRA-HIGH PERFORMANCE FIBER REINFORCED CONCRETE PART 2-TENSILE STRESS-STRAIN RESPONSE. RILEM Publications SARL.

[6] Gebuhr G., Pise M., Anders S., Brands D. and Schröder J., 2022. Damage Evolution of Steel Fibre-Reinforced High-Performance Concrete in Low-Cycle Flexural Fatigue: Numerical Modeling and Experimental Validation. *Materials (Basel)*; **15**.

[7] Pise M., Brands D., Schröder J., Gebuhr G. and Anders S., 2023. Phenomenological material model for damage in steel-fiber reinforced high performance concrete during low cycle fatigue. *Proc. Appl. Math. Mech;* **22**.

[8] Gebuhr G., Anders S., Pise M., Sahril M., Brands D. and Schröder J., 2019. Deterioration development of steel fibre reinforced high performance concrete in low-cycle fatigue. In: *Current Perspectives and New Directions in Mechanics, Modelling and Design of Structural Systems*; Zingoni, Alphose(ed). CRC Press; pp. 1444–1449.

[9] Gebuhr G., Anders S., Pise M., Brands D. and Schröder J., 2022. Damage development of steel fibre reinforced high performance concrete in high cycle fatigue tests. In: *Current Perspectives and New Directions in Mechanics, Modelling and Design of Structural Systems*; Zingoni, Alphose(ed). London: CRC Press; pp. 1327–1332.

[10] Miner M.A., 1945. Cumulative Damage in Fatigue. *Journal of Applied Mechanics*; **12**:A159-A164.

[11] Paris P. and Erdogan F., 1963. A Critical Analysis of Crack Propagation Laws. *Journal of Basic Engineering*; **85**:528–33.

[12] Lanwer J.-P. and Empelmann M., 2021. Fundamental Investigations on the Performance of Micro Steel Fibres in Ultra-High-Performance Concrete under Monotonic and Cyclic Tensile Loading. *Applied Sciences*; **11**:9377.

[13] González D.C., Mena Á., Ruiz G., Ortega J.J., Poveda E. and Mínguez J. et al., 2023. Size effect of steel fiber–reinforced concrete cylinders under compressive fatigue loading: Influence of the mesostructure. *International Journal of Fatigue*; **167**:107353.

[14] de Smedt M., Vandewalle L., de Wilder K., Verstrynge E., 2021. Cyclic Behaviour of Steel Fibre Reinforced Concrete with Acoustic Emission-based Multi-scale Analysis [Ph.D Thesis]: KU Leuven.

[15] Basaldella M., Oneschkow N. and Lohaus L., 2021. Influence of the specimen production and preparation on the compressive strength and the fatigue resistance of HPC and UHPC. *Mater Struct*; **54**.

[16] Basaldella M., Jentsch M., Oneschkow N., Markert M. and Lohaus L., 2022. Compressive Fatigue Investigation on High-Strength and Ultra-High-Strength Concrete within the SPP 2020. *Materials (Basel)*; **15**.

[17] Gebuhr G., Pise M., Sarhil M., Anders S., Brands D. and Schröder J., 2019. Analysis and evaluation of the pull-out behavior of hooked steel fibers embedded in high and ultra-high performance concrete for calibration of numerical models. *Structural Concrete*; **20**:1254–64.

[18] Bates D.M, 1988. Nonlinear regression analysis and its applications. New York: Wiley.